

Supporting Information

Mechanistic Insight toward the Roles of Anions and Cations in the Degradation of Poly (ethylene terephthalate) Catalyzed by Ionic Liquids

Zhaoyang Ju^{a,b}, Lei Zhou^b, Xingmei Lu^b, Yao Li^b, Xiaoqian Yao^{b*}, Shenyu Cheng^a,
Gangwei Chen^c, Chengsheng Ge^{a*}

*(^aCollege of Chemical & Material Engineering, Quzhou University, Quzhou 324000,
P. R. China*

*^bCAS Key Laboratory of Green Process and Engineering, Beijing Key Laboratory of
Ionic Liquids Clean Process, State Key Laboratory of Multiphase Complex Systems,
Institute of Process Engineering, Chinese Academy of Sciences, Beijing 100190, P. R.
China*

*^cZhejiang Zeyi Environmental Protection Technology Co., Ltd, Quzhou 324000, P. R.
China)*

*Corresponding author: xqyao@ipe.ac.cn (X. Yao); gechengsheng@qzc.edu.cn (C. Ge)

Number of Pages: 14

Number of Tables: 6

Number of Figures: 16

Contents

1. Fig. S1: Molecular formula of PET and structure of dimer.
2. Fig. S2-S3: Conformational isomers of Dimer and structures of cations and anions.
3. Fig. S4: The electrostatic potential surface of Dimer, EG anions, and cations.
4. Fig. S5: The optimized configurations of Dimer-OAc/Dimer-Bmim and energies.
5. Table S1: The optimized bond length and Mulliken atomic charge of dimer at M06-2X-D3/ 6-311+G** level.
6. Fig. S6: Optimized reactant, TS, and product structures for the glycolysis of PET with EG corresponding to Scheme 1.
7. Fig. S7: The optimized structure between dimer and EG and relative energies.
8. Fig. S8: Optimized reactant, TS, and product structures for the glycolysis of PET to BHET catalyzed by different anions at different sites.
9. Table S2: The calculated relative energies for the glycolysis of PET to BHET catalyzed by different anions at different sites.
10. Fig. S9: The optimized interaction conformers and energies between anion/cation and PET/EG.
11. Fig. S10: Optimized reactant, TS, and product structures for the glycolysis of PET to BHET catalyzed by different cations at different sites.
12. Table S3: The calculated relative energies for the glycolysis of PET to BHET catalyzed by different cations at different sites.
13. Fig. S11-S15: Optimized reactant, TS, and product structures for the glycolysis of PET to BHET catalyzed by different ILs at different sites.
14. Table S4: The calculated relative energies for the glycolysis of PET to BHET catalyzed by different ILs at different sites.
15. Fig. S16: Optimized the structures of PET, N₁₁₁₁Cl, and EG complexes.
16. Table S5: Changes in bond length for EG in PET, N₁₁₁₁Cl, and EG system.
17. Table S6: The calculated Mulliken atomic charges for EG in PET, N₁₁₁₁Cl, and EG system.

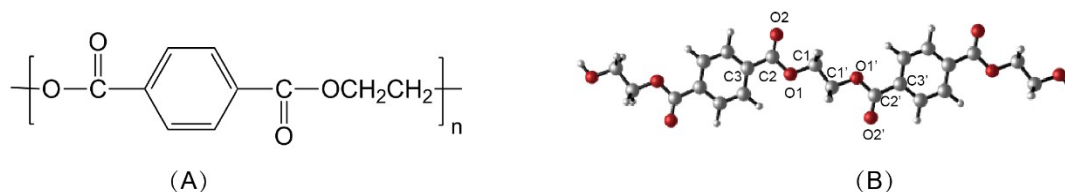


Fig. S1 (A) Molecular formula of PET and (B) the structure of dimer.

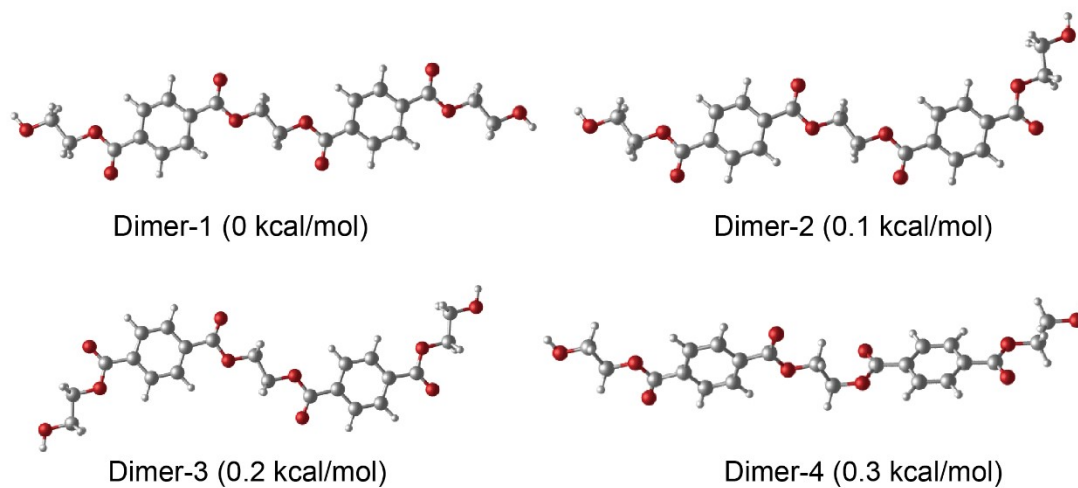


Fig. S2 Conformational isomers of Dimer model compound and the relative energies to Dimer-1 are labeled in parentheses.

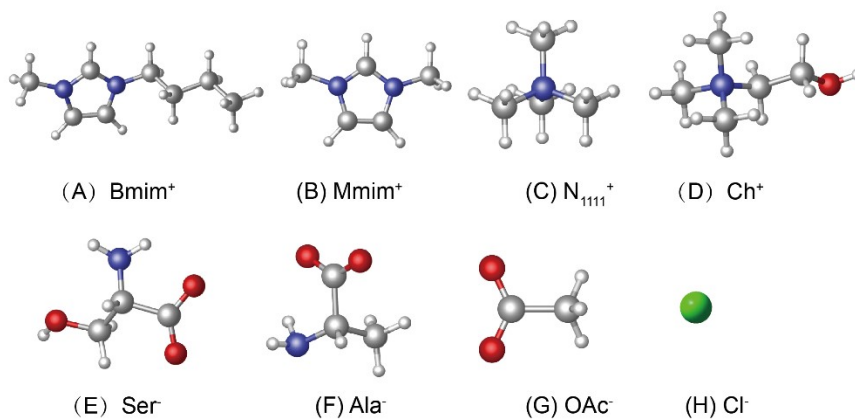


Fig. S3 The structures of (A-D) cations and (E-H) anions optimized at M06-2X-D3/6-311+G** level.

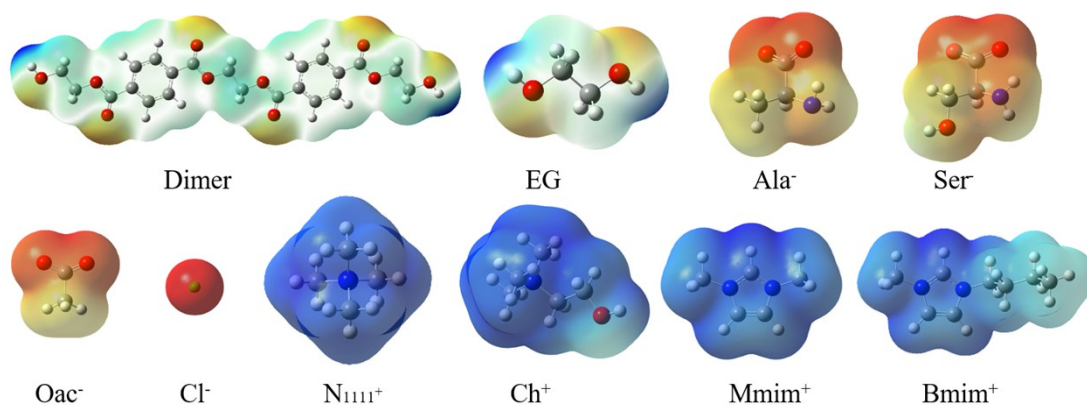


Fig. S4 The electrostatic potential surface of Dimer, EG anions, and cations.

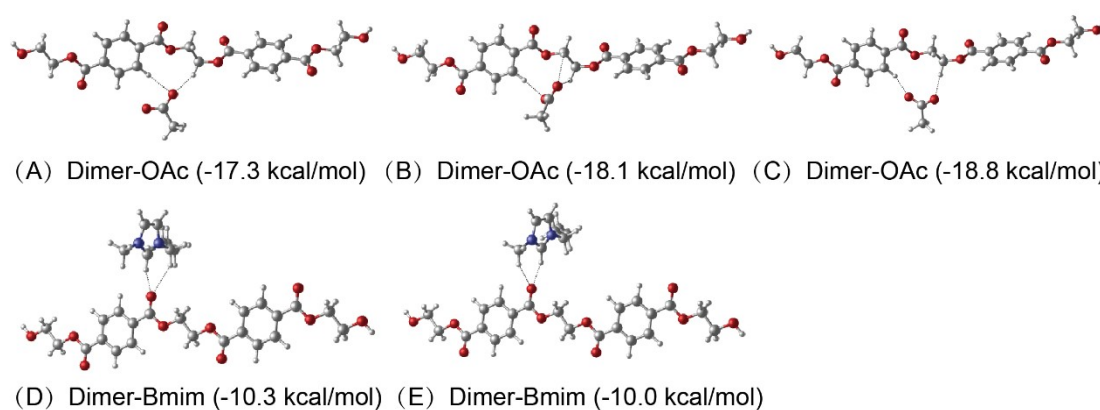


Fig. S5 The optimized configurations of Dimer-OAc and Dimer-Bmim and interaction energies. The hydrogen bonds are indicated by dashed lines. (*RSC Adv.*, 2018, 8, 8209–8219)

Table S1 The optimized bond length and Mulliken atomic charge of dimer at M06-2X-D3/ 6-311+G** level.

Bond	Length (Å)	Bond	Length (Å)	Atom	Charge (a.u.)	Atom	Charge (a.u.)
C3-C2	1.49242	C3-C2	1.49242	C3	0.381	C3'	0.381
C2-O2	1.20134	C2-O2	1.20134	C2	-0.041	C2'	-0.041
C2-O1	1.34378	C2-O1	1.34378	O2	-0.257	O2'	-0.257
O1-C1	1.42832	O1-C1	1.42833	O1	-0.053	O1'	-0.053
C1-C1'	1.51213			C1	0.022	C1'	0.022

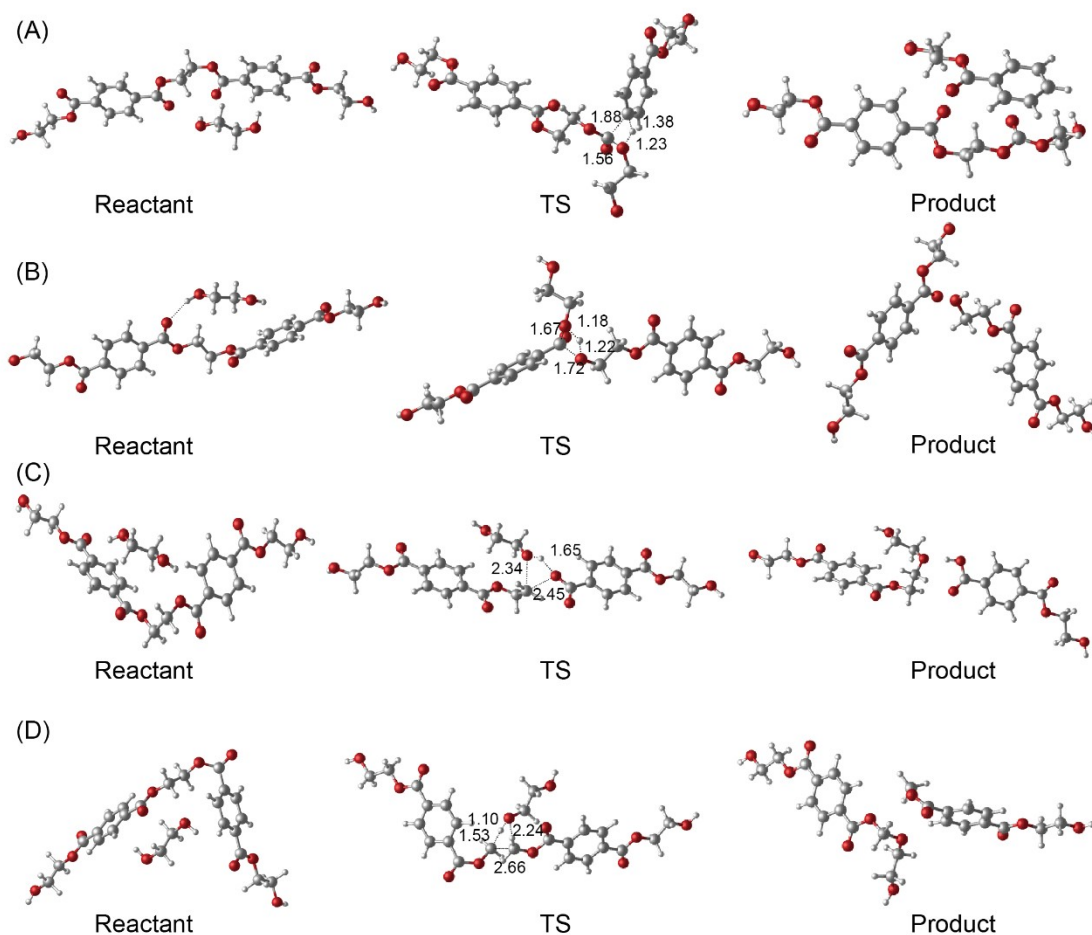


Fig. S6 Optimized reactant, TS, and product structures for the glycolysis of PET with EG corresponding to Scheme 1 (A) path1, (B) path2, (C) path3, (D) path4. Distances are in angstroms.

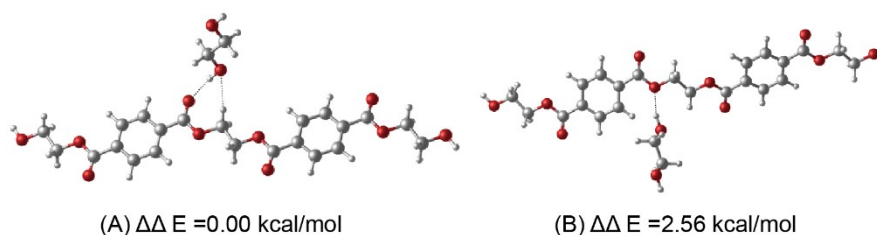


Fig. S7 The optimized structure between dimer and EG and relative energies (A) EG attacks the carbonyl oxygen of dimer (B) EG attacks the ester group oxygen of dimer.

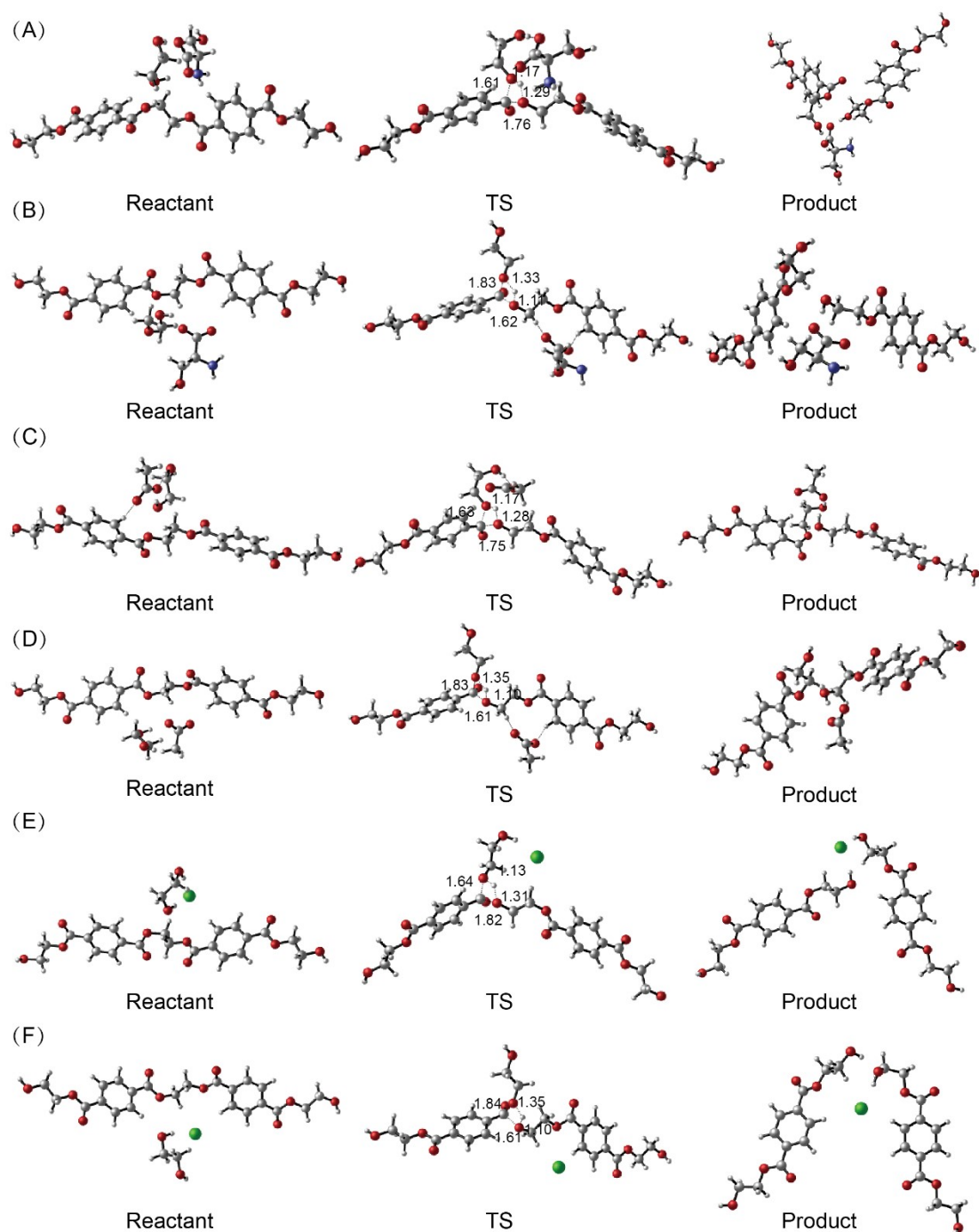


Fig. S8 Optimized reactant, TS, and product structures for the glycolysis of PET to BHET catalyzed by different anions at different sites (A) 1-Ser, (B) 2-Ser, (C) 1-OAc, (D) 2-OAc, (E) 1-Cl, and (F) 2-Cl. Distances are in angstroms.

Table S2 The calculated relative energies (kcal/mol) for the glycolysis of PET to BHET catalyzed by different anions at different sites at M06-2X-D3/6-311+G** level (E_a -activation energy, E_r -reaction energy).

Entry	Catalysts	In vacuo		Ethylene glycol	
		E_a	E_r	E_a	E_r
(A)	Ser ⁻	53.9	5.9	52.9	6.4
(B)		62.6	-0.2	54.8	-2.2
(C)	OAc ⁻	54.3	6.8	52.3	5.8
(D)		64.2	-3.4	55.3	-5.4
(E)	Cl ⁻	52.1	-3.6	51.7	-2.0
(F)		62.7	-8.5	52.0	-7.2

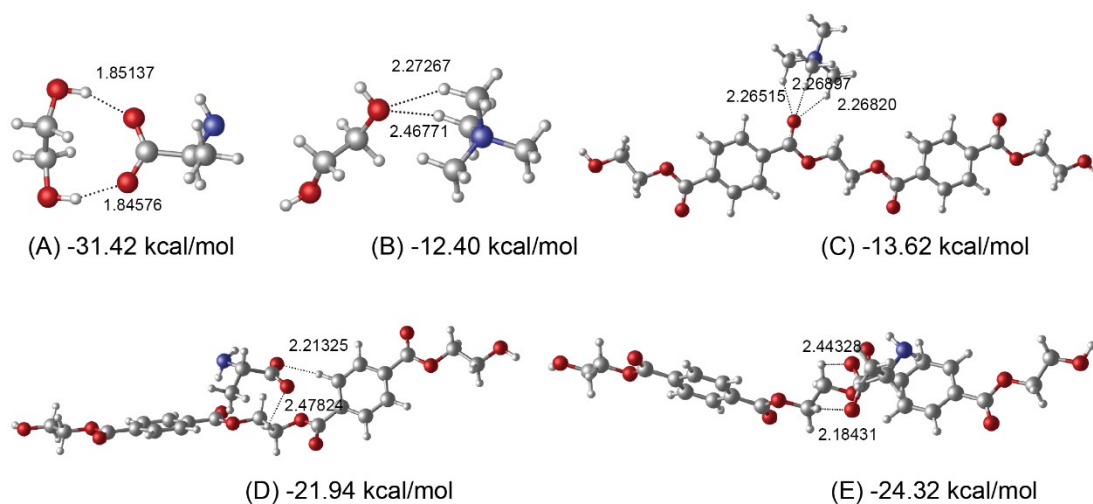


Fig. S9 The optimized interaction conformers and energies corrected by BSSE (A) Ala-EG (B) N₁₁₁₁⁺-EG (C) Dimer-N₁₁₁₁⁺ (D-E) Dimer-Ala⁻ at M06-2X-D3/6-311+G** level.

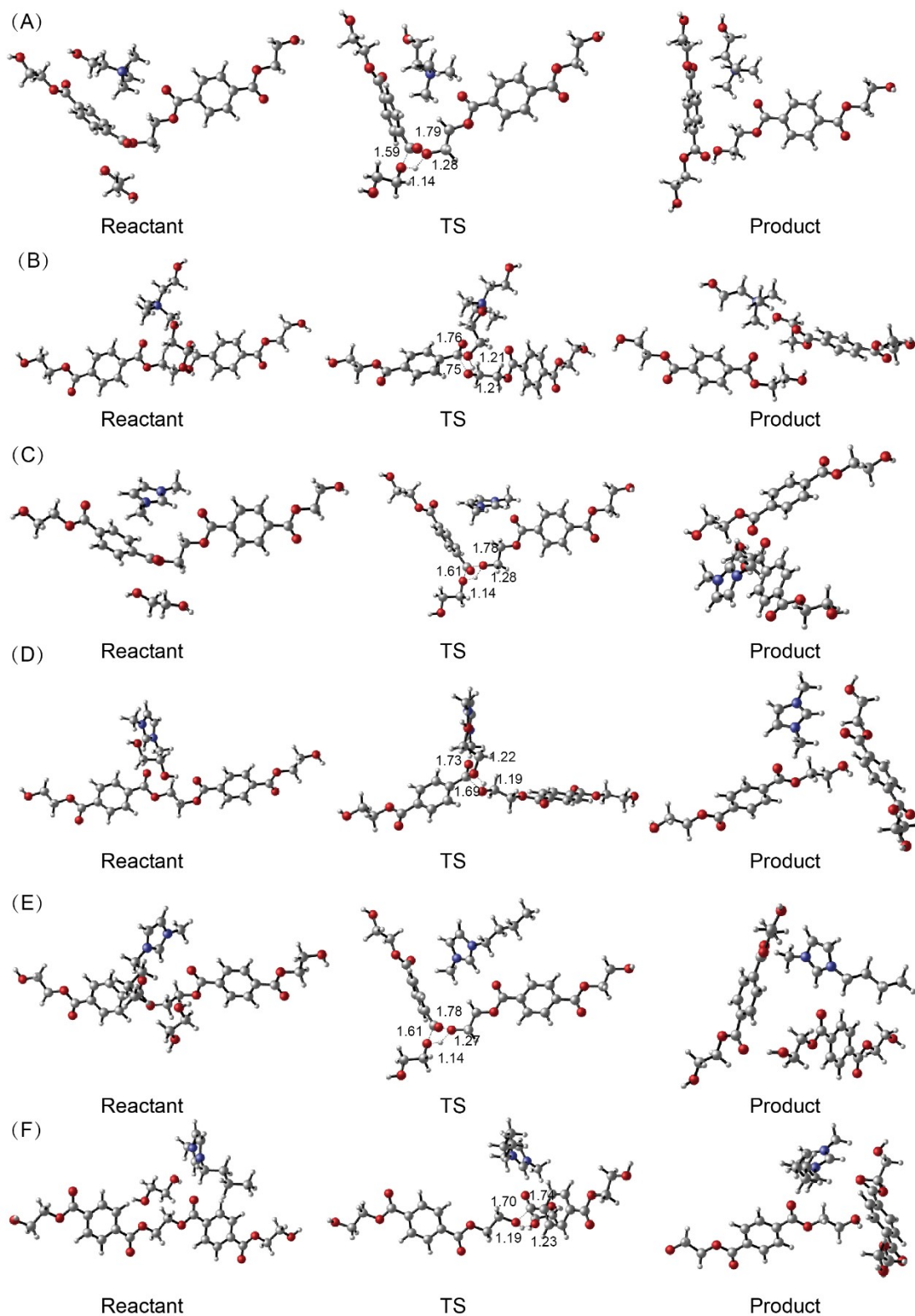


Fig. S10 Optimized reactant, TS, and product structures for the glycolysis of PET to BHET catalyzed by different anions at different sites (A) 1-Ch, (B) 2-Ch, (C) 1-Mmim, (D) 2-Mmim, (E) 1-Bmim, and (F) 2-Bmim. Distances are in angstroms.

Table S3 The calculated relative energies (kcal/mol) for the glycolysis of PET to BHET catalyzed by different cations at different sites at M06-2X-D3/6-311+G** level (Ea-activation energy, Er-reaction energy).

Entry	Catalysts	In vacuo		Ethylene glycol	
		Ea	Er	Ea	Er
(A)	Ch ⁺	40.3	-16.3	42.0	-12.9
(B)		49.2	2.6	48.4	-3.5
(C)	Mmin ⁺	42.2	-10.7	44.8	-11.6
(D)		45.6	-0.4	45.8	-0.5
(E)	Bmim ⁺	46.5	-2.1	46.3	-2.2
(F)		47.2	-8.9	46.7	-5.8

Experiments

Materials

PET pellets (2.0× 2.5× 2.7 mm) were purchased from Jingdong Commercial Co., Jiangsu Province, China. The pellets were ground into 40-60 mesh by a small grinding miller (ZN-02). BmimCl, ChCl, N₁₁₁₁Cl, EG, and the other reagents were purchased from Sinopharm Chemical Reagent Beijing Co., China. All reagents were used as purchased without further purification.

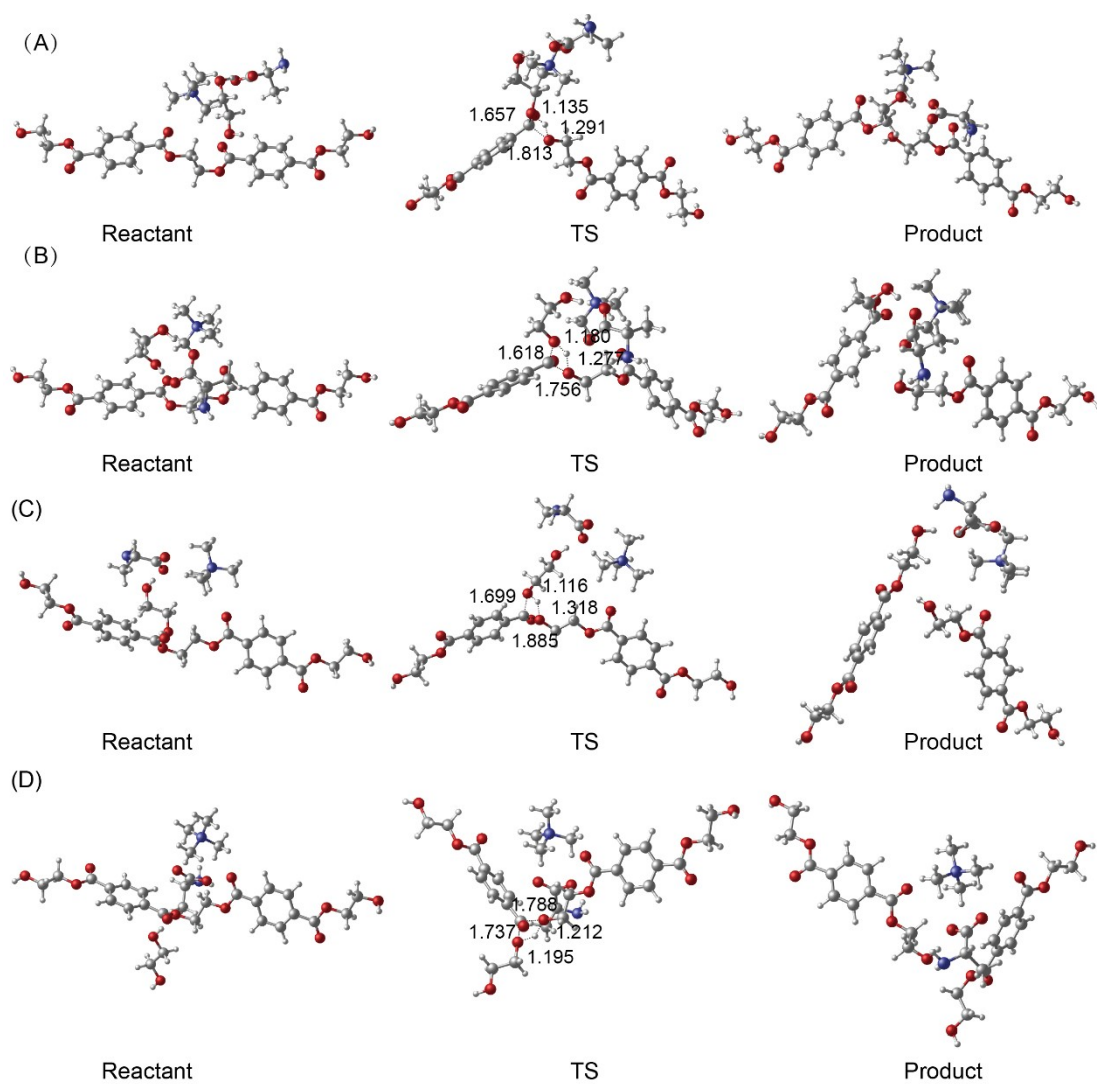


Fig. S11 Optimized reactant, TS, and product structures for the glycolysis of PET to BHET catalyzed by N₁₁₁₁Ala (A-D) at different sites. Distances are in angstroms.

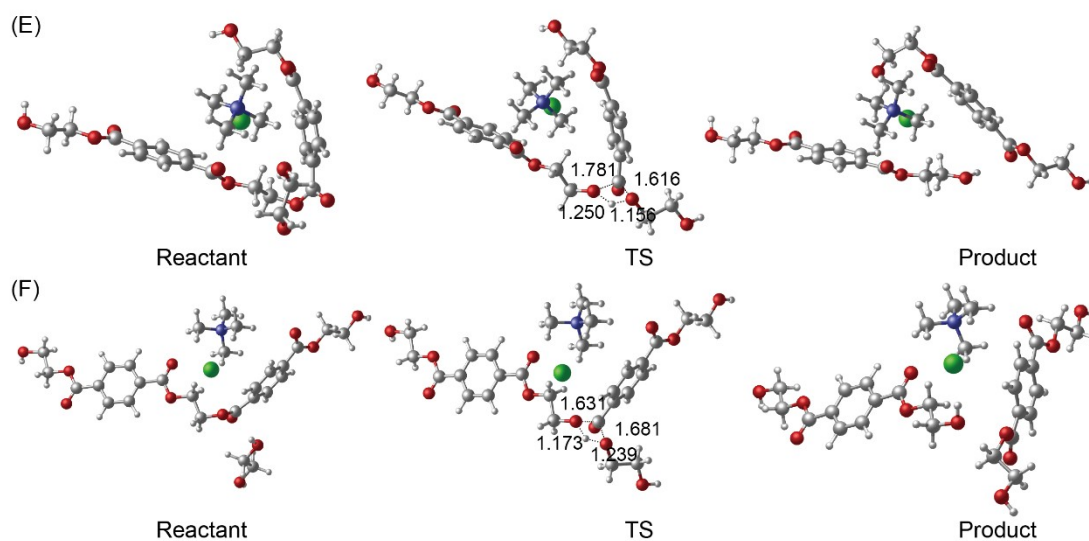


Fig. S12 Optimized reactant, TS, and product structures for the glycolysis of PET to BHET catalyzed by N₁₁₁₁Cl (E-F) at different sites. Distances are in angstroms.

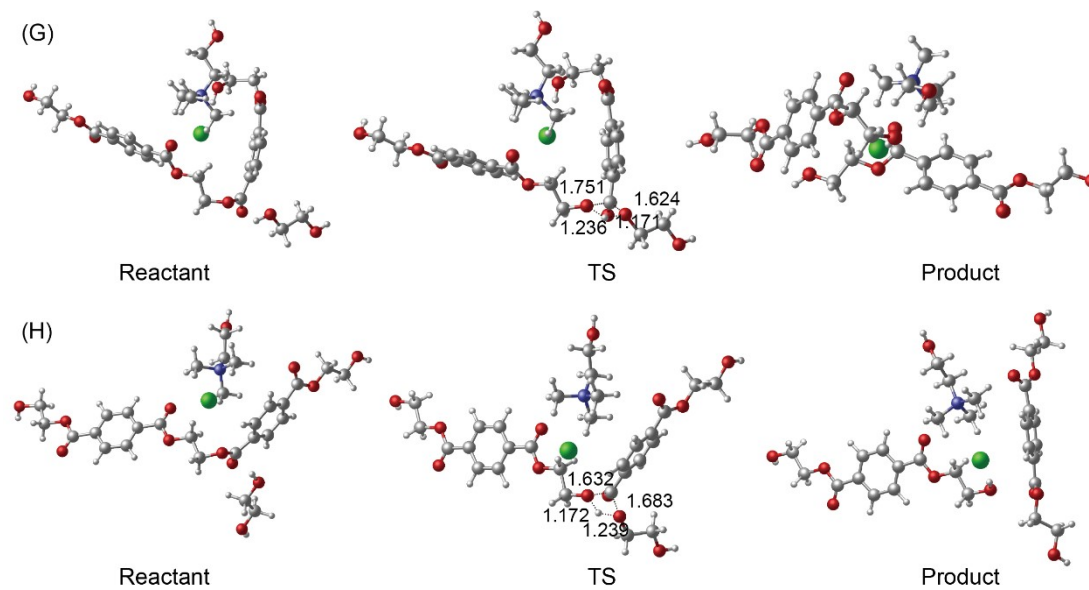


Fig. S13 Optimized reactant, TS, and product structures for the glycolysis of PET to BHET catalyzed by ChCl (G-H) at different sites. Distances are in angstroms.

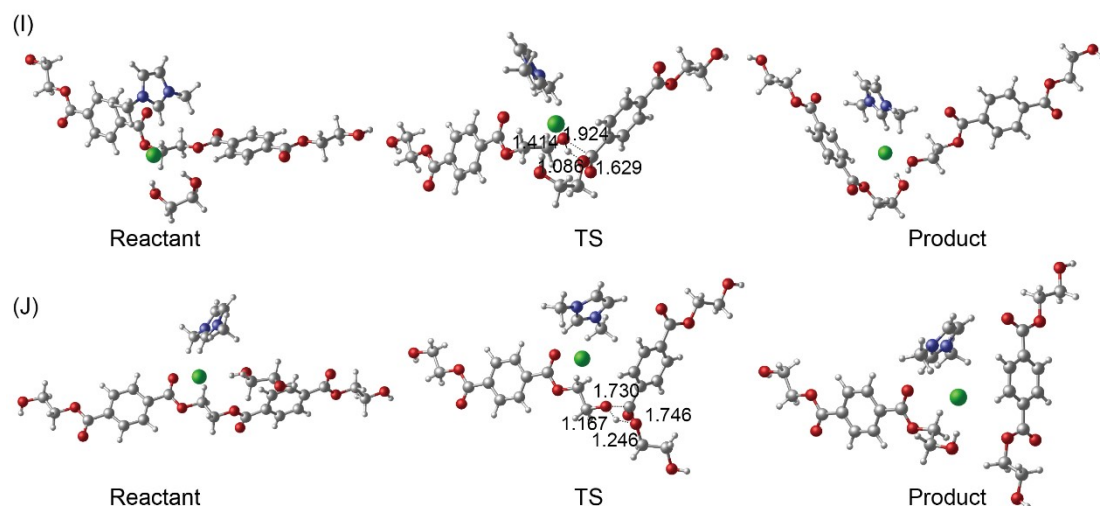


Fig. S14 Optimized reactant, TS, and product structures for the glycolysis of PET to BHET catalyzed by MmimCl (I-J) at different sites. Distances are in angstroms.

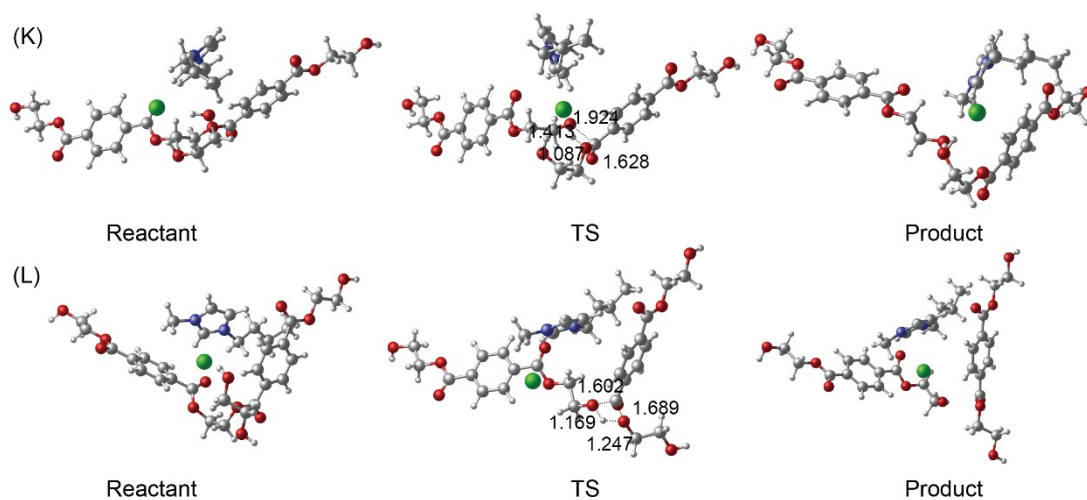


Fig. S15 Optimized reactant, TS, and product structures for the glycolysis of PET to BHET catalyzed by BmimCl (K-L) at different sites. Distances are in angstroms.

Table S4 The calculated relative energies (kcal/mol) for the glycolysis of PET to BHET catalyzed by different ILs at different sites at M06-2X-D3/6-311+G** level (Ea-activation energy, Er-reaction energy).

Entry	Catalysts	In vacuo		Ethylene glycol	
		Ea	Er	Ea	Er
(A)	N ₁₁₁₁ Ala	52.5	0.6	52.2	-0.1
(B)		53.6	5.2	52.8	6.0
(C)		50.0	-0.3	51.8	0.7
(D)		41.5	-15.3	42.8	-8.8
(E)	N ₁₁₁₁ Cl	42.4	-14.9	44.6	-7.3
(F)		47.2	-18.1	46.9	-14.5
(G)	ChCl	43.4	-14.6	44.9	-7.5
(H)		54.9	-7.0	53.5	-6.3
(I)		MminCl	43.9	-9.8	47.4
(J)	BmimCl	49.8	-6.4	47.6	-4.1
(K)		48.1	-5.0	49.9	-4.3
(L)		57.2	-4.4	53.8	-1.5

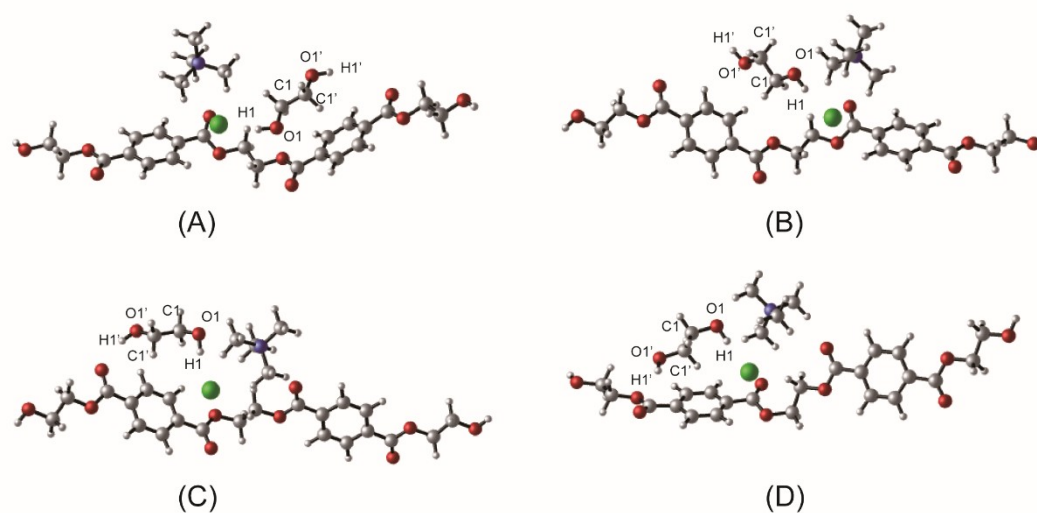


Fig. S16 Optimized the structures of PET, N₁₁₁₁Cl, and EG complexes at different sites.

Table S5 Changes in bond length for EG in PET, N₁₁₁₁Cl, and EG system. Distances are in angstroms.

Bond	EG	A	B	C	D
O1-H1	0.95857	0.97524	0.97676	0.97789	0.98688
O1-C1	1.41714	1.40661	1.40949	1.41414	1.41540
C1-C1'	1.51335	1.51676	1.51488	1.52006	1.52330
C1'-O1'	1.41714	1.42310	1.41948	1.41486	1.41887
O1'-H1'	0.95857	0.95931	0.95937	0.96477	0.96283

The interaction of ILs and EG makes the electronegativity of oxygen of hydroxyl in EG stronger. The Mulliken atomic charges of EG-N₁₁₁₁Cl at different sites corresponding to Fig. S16 are summarized in Table S6. The interaction of anion, cation, and EG make the electronegativity of oxygen of hydroxyl in EG stronger than that of before interaction (from -0.335 to about -0.200 a.u.), which make the oxygen in EG prefer to attacking the carbon of the ester group in PET and finally results in degradation of PET.

Table S6 The calculated Mulliken atomic charges for EG in PET, N₁₁₁₁Cl, and EG system. (unit in a.u.)

Atom	EG	A	B	C	D
H1	0.259	0.307	0.250	0.145	0.137
O1	-0.335	-0.202	-0.228	-0.187	-0.252
C1	-0.257	-0.045	-0.518	-0.157	-0.515
C1'	-0.257	-0.625	-0.260	-0.512	-0.122
O1'	-0.335	-0.242	-0.273	-0.324	-0.154
H1'	0.259	0.247	0.264	0.310	0.228